doi.org/10.36721/PJPS.2024.37.3.REG.523-540.1

Gastro protective natural polymer aided triple drug therapy to eradicate *Helicobacter pylori*

Rajeshpavan Ampapuram[1]*, Gopinath Subramaniyan[2], Ramakrishnan Subburaya Rajendran[3] and Ramakrishna Reddy Padamala[4]

[1]Research scholar, Department of Pharmaceutics, Sri Ramachandra Institute of Higher Education and Research (Deemed to be University), Porur, Chennai, Tamil Nadu, India
[2]Department of Pharmaceutics, Faculty of Pharmacy, Sri Ramachandra Institute of Higher Education and Research Deemed to be University), Porur, Chennai, Tamil Nadu, India
[3]Department of General Medicine, Sri Ramachandra Institute of Higher Education and Research (Deemed to be University), Porur, Chennai, Tamil Nadu, India
[4]Department of Pharmaceutics, Balaji College of Pharmacy, Ananthapuramu Andhra Pradesh, India

Abstract: The core intent of the existing effort was to explore a triple therapy to eradicate *Helicobacter pylori*. A hard gelatin capsule filled with metronidazole (MNZ) floating microspheres aided with *Plantago ovata* seed mucilage (POSM) and Clarithromycin (CMN) floating microspheres aided with *Abelmoschus esculentus* fruit mucilage (AEFM). These mucilages were adopted as they have gastro-protective actions. These microspheres were designed by a central composite design. The influence of polymers used was checked towards the drug entrapment efficacy and floating time was tallied as a response. The capsule also contains Pantoprazole sodium (PZS) enteric-coated mini-tablets. These mini-tablets were checked for the coating thickness as a response (Design Expert). The microspheres and the mini-tablets were gauged for tests and a positive response was reported. The study summarizes that microspheres of MNZ & CMN and PZS enteric-coated mini-tablets can be used to eradicate H. pylori effectively. POSM and AEFM can aid MNZ and CMN microspheres formulations and have ulcer-curing and gastric-protective abilities.

Keywords: Design, floating, *Helicobacter pylori*, microspheres, ulcers.

INTRODUCTION

Helicobacter pylori (*H. pylori*) contagion is the cause of chronic active gastritis, intestinal ulcers, and gastric cancer. This bacterium has evolved to colonize the human stomach (Charitos *et al.,* 2021). Although roughly 20% of these bacteria are in intimate contact with epithelial cells, the most common of them live in the stomach mucus layer (Khan and Alishah, 2022). The key issues with *H. pylori* eradication are claimed to include antimicrobial resistance, patients' deprived acquiescence to antibiotic treatment, and medicine-linked side effects (Cardos *et al.,* 2021). Several medications are in use, including antibacterial Clarithromycin (CMN), antiprotozoal metronidazole (MNZ), and pantoprazole sodium (PZS), a proton pump inhibitor employed in the study (Kan *et al.,* 2020; Moussa, 2017).

CMN is an antibiotic that destroys a wide variety of microbes, atypical pathogens, and some anaerobes (Schubert *et al.,* 2022). When *H. pylori* strains are resistant to other medications in the same category, certain examinations have confessed that CMN has significant *in vitro* action against them. CMN pierces the microbial cell wall and impasses oppositely to sphere V of the 23S ribosomal RNA, hindering aminoacyl transfer RNA and polypeptide creation. Regardless of its fast absorption throughout the gut, *H. pylori*.

*Corresponding author: e-mail: rajeshpavanatp@gmail.com

MNZ is an antiprotozoal that works in anaerobic conditions. The medicine pierces microbial cells and creates a vigorous creation afterward lowering the nitro group, resulting in DNA damage, in the process of passive diffusion (Gong *et al.,* 2021).

To completely eradicate *H. pylori*, strong antibiotic concentrations must be upheld in the stomach mucosa for a protracted spell. This might be accomplished by creating gastroretentive floating microspheres (GRFM) forms that assure persistent medication discharge near the bacterium's biological habitat (El Nashar *et al.,* 2017).

The density of GRFM in the stomach, allows them to stay raft in the stomach for longer spells deprived of impacted by the gastric evacuating rate. The medicine is sluggishly withdrawn from the system at the proper rate. The common of the previously described singular units were pills/ capsules (Chinthaginjala *et al.,* 2021), whereas, multiple units of them (pellets/mini-tablets) have more foreseeable medicine discharge, devoid of localized line damage and the capability to administer units with diverse discharge outlines (Harsha *et al.,* 2020).

Natural polymers can be included in the preparation at a lower cost and with widespread support because synthetic polymers are difficult to come by, expensive and labor-intensive to produce. The researchers were involved to find a natural polymer that may be employed as both a

stomach protective and a discharge modernizer. In the exploration of GRFM, the authors used AEFM (*Abelmoschus esculentus* fruit mucilage) (Okra). AEFM has been verified to be effective on *H. pylori* and has a healing impact on stomach/peptic ulcers (Das *et al.,* 2019; Islam, 2019; Liu *et al.,* 2018). The goal of CMN *Abelmoschus* floating microspheres (CAFM) is to achieve systemic availability in a stable state. Because they are easy to use, controlled liberation systems are a great solution for drugs that have a short half-life or persistent pharmaceutical discharge.

POSM (*Plantago ovata* seed mucilage) (Isabgol) was used in the exploration of MNZ- POSM floating microspheres (MPFM). POSM has been confirmed to be effective on *H. pylori* and has a healing impact on stomach/peptic ulcers (Keshavarzi *et al.,* 2021; Shapla *et al.,* 2018). MPFM seeks to conserve systemic availability at all times. Precision liberation systems are an excellent answer for medications that are short-acting or entail persistent medicating because they are simple to use.
The combined use of MNZ and clarithromycin involves their synergistic effects in treating bacterial infections, particularly in instances where a broad spectrum of microorganisms is targeted. Metronidazole, characterized by a nitroimidazole structure, acts through intracellular reduction, generating reactive intermediates that disrupt DNA, ultimately causing cell death. CMN, a macrolide antibiotic, inhibits bacterial protein synthesis by binding to the 50S ribosomal subunit. While the specific interaction mechanisms between these two drugs may not entail direct chemical interactions, their combined use is strategically employed to combat a variety of bacterial infections. The pH-dependent nature of these antibiotics is noteworthy, with metronidazole demonstrating optimal absorption in the acidic stomach environment. Although clarithromycin absorption may be influenced by food intake, it is not as strongly pH-dependent. This multidrug regimen is prescribed based on the complementary actions of these antibiotics against different types of microorganisms, and any adjustments to these practices should consider the latest medical insights and professional advice.

The enteric-coated dosage forms (ECDF) discharge the medicament after reaching the neutral countering portion of the duodenum, GRFM has the best defense on unhinged drugs at lesser pH. By providing fast discharge in the duodenum while still providing continued input of pharmaceuticals with an absorption window, the ECDF of PZS may revamp the bioavailability.

The most effective conquerors of the stomach acid ooze are suppressors of the gastric H+ and K+-ATPase (Aby *et al.,* 2020; Spugnini and Fais, 2020). These drugs lower acid production (basal and stimulated) by 80 % to 95 % in usual doses. Individuals with peptic ulcers and GERD should focus on symptom relief, disease prevention and ulcer repair as their primary therapy goals. PZS is a swapped benzimidazole imitative that blocks acid proton pumps in the stomach, which are the ultimate common mechanism for acid emission. For a long time, the medication binds covalently to the proton pumps, hindering stomach acid discharge. However, the medication irritates the gastrointestinal mucosa, which can produce nausea and vomiting. PZS's stability rapidly deteriorated in the stomach's acid medium, although it is acceptable under alkaline settings. As a result, PZS should be given to the intestine. As a result, turning PZS into an ECDF could fix the drug's stomach stability problem while also allowing it to be discharged into the intestine. The major goals of this study were to use the direct compression method to make and analyze the ECDF of PZS, to choose an opposite coat to construct the dosage form, and to resist drug squalor by the stomach contents and the acidic environment (Krag *et al.,* 2018).

Customary exploration engrossed on one wavering at a time due to the difficulties of deploying one wavering at a time. All of these features cannot be considered at the same time due to statistical restrictions. All of these wavering will be intertwined, resulting in incorrect outcomes. The design of trials is an imperative part of multivariate analysis (DOE). Incomplete issues are taken into account in DOE. Screening and optimization are the goals of DOE (Ahad *et al.,* 2019). The components in A and FD are combined in every way feasible. In terms of level, FD is either "high" (+1) or "low" (-1). The FM of MNZ in this exploration was analyzed by design expert software (Ahad *et al.,* 2021; Hindustan *et al.,*2012).

MATERIALS AND METHODS

Materials

Waksman Selman Pharmaceutical Limited, Anantapur, donated clarithromycin, metronidazole and pantoprazole sod. Local vendors provided *Plantago ovata* seeds and *Abelmoschus esculentus* fruits. Merck, Hyderabad, provided sodium alginate, $CaCl_2$, croscarmellose sodium, microcrystalline cellulose, talc, magnesium stearate and cellulose acetate phthalate.

Experimental design for making GRFM

Using Design-Expert software (11.0.5.0, Stat-Ease, Inc.), a 9-run central composite design (CCD) was used in this study design. By tracking their key, boundary and quadratic chattels, this approach is intended to predict independent wavering (X) $B_0+B_1\ X_1+B_2X_2+B_{12}X_1X_2+B_1X_{12}+B_2X_{22}$ and $B_0+B_1\ X_1+B_2X_2+B_{12}X_1X_2+B_{12}X_1X_2+B_{12}X_1X_2+\ B_{12}X_1X_2+Y$ is the dependent (Y) and X_1 and X_2 were the independent wavering and B_0, B_1 and B_2 are the regression coefficients (table 1).

Preparation of GRFM

Using a syringe and needle, 2% $CaCl_2$ was applied as drops and SA, MNZ and POSM solutions were combined while being persistently stirred (IKA-R1385) at 500 rpm

for 10 min. Glutaraldehyde solution was applied drop by drop and swirled for 15 minutes (Ismail *et al.,* 2022; Sowjanya *et al.,* 2022). MPFM was stored in a vacuum desiccator later on Whatman filtration and dried out (at 40ºC for 2h) (table 2). By substituting POSM with AEFM, the same method was used to create CAFM (table 3).

Preparation of PZS tablets

A rotating tablet compression machine (Kelweka) and concave punches with an 8 mm diameter were employed. A proper granular mixture was trampled into tablets weighing around 100mg and holding 40mg of PZS (Ahmad *et al.,* 2022; Maderuelo *et al.,* 2019), which were then stored in an airtight vessel (table 4).

PZS tablet coating

Making of an enteric coating solution

Eudragit L100 (EL100) (X_1) and cellulose acetate phthalate (CAP) (X_2), a PEG 1.5% w/w plasticizer, were combined to form an enteric polymer combination, which was then liquefied in acetone. The remaining solvent combination was then used to make up the volume, the solution was added and this mixture was stirred continuously for one hour at 1000 rpm with a paddle motorized stirrer. The stirred solution was then cleared with muslin fabric to yield the solution (table 5) (Le *et al.,* 2021).

Making PZS enteric-coated tablets

The solution of the EC polymer was used to coat the tablets (EL100 or CAP). The dipping went well and the desired tablet coating was applied, resulting in a weight gain. Weight variation, thickness, PZS content and an *in vitro* dissolving study of coated tablets were all gauged (Chen *et al.,* 2021). The final scheme of the hard gelatin capsule fill holds GRFM (≡CMN 250 mg and ≡MNZ 250mg) and an ECDF of PZS (fig. 1),

Evaluation of GRFM

Melting point

To check the purity of MNZ, CMN and PZS, the open capillary method was employed to establish their identification/purity by their melting points.

Drug excipient suitability studies

The blends were combined (1:1) in a DSC micro pan and scanned at 50-300°C (Venchal Scientific-412105-USA). The cooperation by uniting MNZ and POSM was explored by FTIR spectroscopy (Bruker) in the 4000-400 cm^{-1} range. Harmony of CMN and AIFM; PZS with excipients was also gauged.

Evaluation of physical properties of GRFM

The particle size (PS) of the MPFM was determined by a stage micrometre. Dry MPFMs were placed on a sanitary glass slide and appraisals were taken with an ocular micro metre. At least 200 times, every batch of MPFMs was counted. CAFM was also tallied in the same way (Rajora and Nagpal, 2022).

Production yield

The weight of MPFM (W_1) has deviated from the dry weight in the piece study (W_2). This output was calculated by dividing every dry MPFM (W_1) by its dry weight (W_2). CAFM was also put to the test (Annepogu *et al.,* 2020).

$$\% \text{ Yield} = \frac{\text{Weight of GRFM}}{\text{Total weight of drug and polymer}} \times 100$$

Entrapment Efficiency

Using 0.1 M HCl, 100 mg of MPFMs were deliquesced in the solution overnight. At 278 nm, the filtrate underwent spectrophotometric analysis (Elico Spectrophotometer, SL-174). EE was governed by the ratio of the definite MNZ in the GRFM to the quantity that was originally introduced. CAFM was tallied similarly at 272nm (Babu *et al.,* 2022).

$$\text{EE} = \frac{\text{Practical yield}}{\text{Theoretical content}} \times 100$$

% Buoyancy Study

100 rpm was used to stir in 900 ml HCl (0.1N), which holds MPFM (100mg), for 8 hours in a type II USP dissolution apparatus. To remove the raft layer from MPFM, it was pipetted and cleared. Filtration was used to separate the raft layer from the sinking particle layer. In a desiccator, both kinds of units were dehydrated and weighed. By the provided formula, the raft was determined for every type of particle (Oladeji *et al.,* 2022).

$$\% \text{ Buoyancy} = \frac{\text{Initial weight of GRFM}}{\text{Weight of GRFM}} \times 100$$

In the same manner, CAFM were also considered.

In Vitro MNZ Discharge Study

The USP-II apparatus was used with 900 ml of HCl (0.1N) at 37±0.5°C and 505 rpm of stirring. At each rest, 5 ml of the dissolving medium was replenished. The same was reclusive and spectrophotometrically appraised at 278 nm. CMN was gauged similarly at 272 nm (Ahmed, 2019; Raza *et al.,* 2019).

Statistical optimization

The study adopted Design-Expert, which creates response surface plots and contour plots (2D) (3D). By arbitrating ANOVA values, it was statistically possible to confirm the polynomial's intended behaviour. The ANOVA bequest produced a statistical model for controlling model profusion and gifting (p-value 0.05). The same criteria were used to measure CAFM (Ahad *et al.,* 2021; Israr *et al.,* 2022).

Evaluation of PZS mini tablet

In vitro drug discharge studies

Using a USP-II, the *in vitro* drug discharge from the GRFM was explored (Electrolab TDT-08L, Mumbai, India). For 2 h, 900 ml of pH 1.2 acidic buffer was used, later by 1 h of pH 6.8 buffer. In the basket, the tablet was stowed. The stirring speed was set to 100 rpm at 37±0.5ºC. Samples were taken out at consistent pauses and swapped with fresh dissolving media. A UV spectrophotometer was used to compare the samples to a blank at 288 nm (Soisuwan *et al.,* 2018; Zhang *et al.,* 2019). The discharge tests were done three times, with the average data plotted versus time.

RESULTS

The overlay spectrum of MNZ aloe and the excipients was as per Fig. 2. Similarly, the FTIR spectrum of CMN alone and its excipient combination (fig. 3) and finally the harmony of PZS with the excipient blend defines the appropriateness of the excipients with the drugs used (fig. 4).

The fit summary of MPFM and CAFM (table 6) and the ANOVA in table 6. The PS, % yield, discharge at 10h and float % of MPFM (fig. 9) and CAFM (fig. 10) were defined. The dissolution in USP- II equipment, the *in vitro* discharge confessed the resists of PZS discharge in acidic media and discharge in alkaline medium (fig. 11).

The interaction outcome (fig. 12), contour and 3D plots (fig. 13) of polymers on the coating thickness of PZS mini-tablets were also illustrated. The flow possessions of the PZS blend were as per table 8.

The constraints of the PZS core tablet were as per table 9. The thickness, weight, solubility, etc., of CAP, eudragit L100, were examined and checked for their solubility in copious pH solutions (table 10). The summary of the output of PC mini-tablets obeyed the quadratic model (table 11).

DISCUSSION

The FTIR spectra confessed that the absorption ranges for CMN alone were 3498.51 cm^{-1} (O-H), 3126.03cm^{-1} (C-H) and 1768.45cm^{-1} (C=O) and they perceived in CMN blend with excipients 3467.16cm^{-1}, 3124.84cm^{-1} and 1784.51cm^{-1}.

The FTIR spectra reveal confessed that the absorption ranges for MNZ alone were 3481.12 cm^{-1} (O-H), 3025.94 cm^{-1} (C-H), and 1701.25 cm^{-1} (C=O) and they see in MNZ blend with excipients 3495.06cm^{-1}, 3065.29cm^{-1} and 1751.34 cm^{-1}.

Whereas the absorption ranges for PZS alone were 3493.62cm^{-1} (O-H), 3090.51cm^{-1} (C-H) and 1721.64cm^{-1} (C=O) and they perceived in PZS blend with excipients 3499.57 cm^{-1}, 3098.88cm^{-1} and 1714.82cm^{-1}.

Using a UV-VIS spectrophotometer, MNZ was identified at 278 nm in a 0.1M HCl solution. The calibration curve for Beer's law was perceived to be between 0 and 10g/ml. Similarly, CMN was appraised at 272 nm in 0.1M HCl and Beer's law was perceived to be between 0 and 10 g/ml.

The fit summary of MPFM displayed the fitting of the model to quadratic with an adjusted regression value of 0.9997 and the predicted 0.9986 for DEE; adjusted vs. predicted regression values of 0.9993 and 0.9975 for FT. Similarly, the fit summary of CAFM disclosed the fitting of the model to quadratic with an adjusted regression value of 0.9999 and the predicted 0.9996 for DEE; adjusted vs. predicted regression values of 0.9977 and 0.9898 for FT.

In the case of MPFM, the F-value of the model is 5408.60, defining that dealing with a substantial model. The F-value for this model is 2167.41. The following is the equation for DEE and % buoyancy. Whereas, CAFM, 11973.00 is the F-value for the model, signifying it is significant. On the other hand, a model F-value of 707.52 signposts that the model is significant.

With a fortuitous of 0.01 %, an F-value of such a big amount is dubious to arise due to noise. Significant terms are those with p-values greater than 0.05. A, B and B_2 are the three most imperative model terms here. The terms with a value greater than 0.10 have no meaning. If there are a lot of irrelevant words, it may be advantageous to decrease model terms.

Diagnostic plots were reviewed and the DEE's high level of accuracy was proved (fig. 2A & B). The studentized residuals (SR) may proclaim an extreme of coloured points defining the DEE near the normal possibility line, signifying that the residuals (RLs) are normal and that the underlying data should be analysed as such. According to the RLs (fig. 2A & 4A). fig. 2B and 4B proclaimed that the facts are off the cook's line, signifying that the variance is persistent. Arrua (2022) and Malladi and Jukanti (2016) and reported comparable findings (Arrua *et al.,* 2022; Malladi *et al.,* 2016).

Diagnostic plots were utilised to gauge the quality of fit of the FT (fig. 2C & D; fig. 4C & D). Normal likelihood plots of rapidly SR proclaimed FT around the normal prospect line, specifying that the RLs were normal and the retort analysis was fit. The RLs in fig. 2C and 4C are consistently distributed because they are straight lines. When plotted against external SR, FT was within its defined bounds. fig. 2D & 4D confirm the continuous variance hypothesis. As directed in the RLs and run facts in the graphic, some wavering influence FT (Thombre and Gide, 2016).

The goodness-of-fit of the DEE and FT was calculated by contour and 3D diagnostic plots (fig. 3A & B for DEE

and fig. 3C&D for FT) and (fig. 5A & B for DEE and fig. 5C&D for FT). The DEE and FT could be visible around the normal possibility line in plots of the normal likelihood of quick SR, subsidiary to the assumption that the RLs were normal and the analysis of rejoinders was proper (Stephin and Marina, 2020).

The M-6 particles were larger than the other MPFM particles, which ranged in size from 34.8±1.84 µm to 45.3±1.84 µm. The range of MPFM yields was 78.9±2.31 to 95.2±3.46%. M-5 (92.1±3.51%) and M-4 (95.2±3.46%) had higher yields, whereas M-1 had the lowest yields. To plan MPFM's dissolution, research was directed in that direction. After 10 h, the comparison of M-6 showed 97.0±4.57% of excellent MNZ discharge. Increased POSM concentration makes its discharge-retarding abilities more obvious. The M-9 had the highest buyback (94.72±5.47%), while the M-3 had the lowest buyout (81.7±2.15%). (Fig. 6). The results showed that MPFMs with higher SA and POSM ratios floated better than those with lower ratios (Paul *et al.,* 2018). The MPFM's small size may be answerable for their inferior float.

Looked into how CMN discharge and FT affected AEFM and SA. PS was calculated using optical microscopy for all GRFM. C-9 particles are larger than CAFM arrays, which have sizes ranging from 38.01±0.9 µm to 48.9±2.11 µm. More yields for CAFM were for C-8 and C-9 and the yield ranged from 82.8 to 92.3.38%. To control CAFM's disintegration, a study was done. At the end of 10h, C-3 and C-2 proclaimed 96.3±3.85% and 93.2±5.37% of excellent CMN discharge, respectively. As AEFM concentration grew, discharge retarding features started to appear (Hardikar and Bhosale, 2018).

The C-1's hover was the lowest (83.85%) and the C-9's was the greatest (94.85%). It was discovered that CAFM with a higher proportion of SA and AEFM had superior buoyant possessions than those with a smaller concentration of these polymers. The CAFM's modest size may be the cause of its inferior drifting. The granules' bulk densities ranged from 0.329±0.01 to 0.781±0.02 g/ml, while their tapped densities were determined to be between 0.359±0.02 to 0.835±0.07 g/ml. The flow features of the granules were gaged by the angle of repose and Carr's Index. Compressibility ratings ranging from 5.766±0.31 to 9.278±0.51% designate flowability. All GRFM had an angle of repose of around and <25º (23.28±0.25 to 26.55±0.32), defining that the granules were flowable (table 8).

The PZS tablets were estimated for hardness, weight variation, content homogeneity, friability and *in vitro* drug discharge (table 9). The product's hardness must be regulated to confirm that it is firm and adequate to handle without breach, but not so hard that it takes too long to disintegrate. The tablets' average hardness was <4kg/cm^2 in the range of 5.32±0.22 to 8.81±0.65 kg/cm^2. The friability value of tablets, which is influenced by their hardness, should be in the 1% range, which is the standard friability range. The friability of the manufactured tablets was perceived to be <1% w/w (Ejeta *et al.,* 2022). The concentration of PZS in tablet format was persistent between 98.07±9.68 to 102.38±8.09%. The average weight ranged from 103.24±3.38 to 106.84±8.58 mg. The time it took for the disintegration to occur ranged from 6.62±0.05 to 12.89±0.08 sec, signifying a successful outcome (table 9).

The appearance, film thickness, weight and solubility and physicochemical properties of cellulose acetate phthalate, EudragitL100, were examined. Eudragit L100, a CAP-based enteric polymer, was publicized to be fully soluble at pH 6.8 and insoluble at pH 1.2.

With USP Type II equipment, the *in vitro* discharge of PZS from the tablets was examined at pH 1.2 for 2 h and then in buffer at pH 6.8 for 1 h (Electrolab TDT-08L, India). The discharge ranged from 80.91±1.5 to 99.85±1.7%, among them the best outcomes were from the PC-1, with PZS discharge beginning at 2 h and peaks at 99.85±1.7% (with 7% of EL100 and CAP) and the least was by PC-6 with 89.95±2.3 (comprise 8.41421% of EL100:CAP). The summary of the retort of PC mini-tablets obeyed quadratic with an adjusted R^2 value of 0.8630 with a p-value of <0.05 (0.0487) (Lin *et al.,* 2015).

The F-value of 11.07 in the model indicates that it is statistically significant. There is a 3.77% possibility that noise will result in an F-value of this magnitude. Model terms that have P-values under 0.05 are noteworthy. In this configuration, the names A, A_2 and B_2 are imperative model terms. If the value is >0.1, the model terms are not mandatory. If your model contains a lot of small-scale terms, model reduction may completely revamp it. The equation for the film thickness was (Y_1) =+0.2200+ 0.0430A+0.0138B-0.0150AB+0.0413A_2 +0.0563B_2.

Examining diagnostic plots revealed that the film thickness was extremely accurate (fig. 9A). The SR may indicate that there are more coloured dots around the normal probability line denoting film thickness, indicating that the RLs are normal and that the underlying data should be interpreted as such. fig. 9A, 9B, 9C and 9D showed that the values were far from the cook's line, indicating that the variation was persistent. Fig. 9D showed comparisons between the real-world results and what was expected, what happened and what was projected. The goodness-of-fit of the film thickness was measured using 3D diagnostic plots (fig. 9E). The film thickness could be seen around the normal prospect line on plots of the normal likelihood of each SR, reinforcing the idea that the RLs were normal and the rejoinder analysis was appropriate. All of the points in fig. 9F expressed a steady running with no very harsh areas because RLs are straight lines and they follow a normal distribution (Gong *et al.,* 2018).

Table 1: Factors ns the responses studied in the making of GRFM

GRFM	Label	Independent variables	Dependent variables
Clarithromycin	CAFM	X_1 (Sod. alginate) and X_2 (POSM)	Y_1 (Entrapment efficacy) (DEE)
Metronidazole	MPFM	X_1 (Sod. alginate) and X_2 (AEFM)	and Y_2 (floating time) (FT)

Table 2: MPFM formulation details

Content	GRFM								
	M-1	M-2	M-3	M-4	M-5	M-6	M-7	M-8	F-9
MNZ	250	250	250	250	250	250	250	250	250
POSM (mg)	50	50	50	75	75	75	100	100	100
$CaCl_2$ (%)	2	2	2	2	2	2	2	2	2
Sodium alginate (mg)	100	150	200	100	150	200	100	150	200
Glutaraldehyde (ml)	0.24	0.24	0.24	0.24	0.24	0.24	0.24	0.24	0.24
Deionized water (ml)	200	200	200	200	200	200	200	200	200

Table 3: Composition of the CAFM

Component	GRFM								
	C-1	C-2	C-3	C-4	C-5	C-6	C-7	C-8	C-9
Clarithromycin	250	250	250	250	250	250	250	250	250
AEFM (mg)	50	50	50	75	75	75	100	100	100
Sodium alginate (mg)	100	150	200	100	150	200	100	150	200
Calcium chloride (%)	2	2	2	2	2	2	2	2	2
Glutaraldehyde (ml)	0.24	0.24	0.24	0.24	0.24	0.24	0.24	0.24	0.24
Deionized water (ml)	200	200	200	200	200	200	200	200	200

Table 4: Composition of ECDF of PZS

Contents (mg)	P-1	P-2	P-3	P-4	P-5	P-6	P-7	P-8	P-9
Pantoprazole sod.	40	40	40	40	40	40	40	40	40
Sod. Starch glycolate	2	4	6	2	4	6	2	4	6
Microcrystalline cellulose	20	20	20	20	20	20	20	20	20
Lactose	34	32	30	34	32	30	34	32	30
Talc	2	2	2	2	2	2	2	2	2
Silica (powdered)	2	2	2	2	2	2	2	2	2
Tablet weight	100	100	100	100	100	100	100	100	100

Table 5: Various formulas of PZS in the study

GRFM	EL100 (X_1) (%)	CAP (X_2) (%)	PEG (ml)	Acetone (ml)
PC-1	6	6	1.5	60
PC-2	8	6	1.5	60
PC-3	6	8	1.5	60
PC-4	8	8	1.5	60
PC-5	5.58579	7	1.5	60
PC-6	8.41421	7	1.5	60
PC-7	7	5.58579	1.5	60
PC-8	7	8.41421	1.5	60
PC-9	7	7	1.5	60

Table 6: Fit summary of the outcomes

MPFM-response 1: DEE (%)			
Source	Sequential p-value	Adjusted R^2	Predicted R^2
Quadratic	< 0.0001	0.9997	0.9986
MPFM- response 2: FT (h)			
Quadratic	0.0020	0.9993	0.9975
CAFM- response 1: DEE (%)			
Quadratic	< 0.0001	0.9999	0.9996
CAFM- response 2: FT (h)			
Quadratic	0.0281	0.9977	0.9898

Table 7: ANOVA for the responses

Source	Sum of Squares	F-value	p-value
MPFM- response 1: DEE (%)			
Model	270.43	5408.60	< 0.0001
A-SA	0.0150	1.50	0.3081
B-POSM	253.50	25350.00	< 0.0001
AB	0.0900	9.00	0.0577
A^2	0.0050	0.5000	0.5305
B^2	16.82	1682.00	< 0.0001
MPFM- response 2: FT (h)			
Model	148.51	2167.41	< 0.0001
A-SA	0.1350	9.85	0.0517
B-POSM	145.04	10584.12	< 0.0001
AB	0.8100	59.11	0.0046
A^2	0.0272	1.99	0.2535
B^2	2.49	181.99	0.0009
CAFM- response 1: DEE (%)			
Model	266.07	11973.00	< 0.0001
A-SA	0.2017	45.38	0.0067
B-AEFM	249.62	56163.37	< 0.0001
AB	0.0000	0.0000	1.0000
A^2	0.0050	1.12	0.3667
B^2	16.25	3655.12	< 0.0001
CAFM- response 2: FT (h)			
Model	16.05	707.52	< 0.0001
A-SA	0.0704	15.52	0.0291
B-AEFM	15.84	3492.09	< 0.0001
AB	0.0025	0.5510	0.5117
A^2	0.0001	0.0306	0.8723
B^2	0.1335	29.42	0.0123

The equation for DEE and FT for MPFM can be uttered as:

- DEE (%) =+79.6-0.05A+6.5B+0.15AB-0.05A_2-2.90B_2
- % Buoyancy= +86.39+0.15A+4.92B+0.45AB+0.1167A_2+1.12B_2

The equation for DEE and FT for CAFM can be stated as:

- DEE (%) =+86.07+0.1833A+6.45B+0.0AB-0.05A_2-2.85B_2
- FT=+11.91+0.1083 A+1.62B+0.025AB+0.0083 A_2+0.2583B_2

The interaction effect of polymers (fig. 2), Contour plot and 3D response plots (fig. 3) on the DEE and the FT for MPFM were illustrated. Plots viewing the interface effect of polymers (fig. 5), Contour plot and 3D response plots (fig. 6) of MPFM and interaction effect of polymers (fig. 7), Contour plot and 3D response (fig. 8) of CAFM on the DEE and the FT were also depicted.

Table 8: Flow abilities of PZS blend

Formulation	Angle of repose (o)	Bulk density (g/ml)	Tapped density (g/ml)	Carr's index (%)	Hausner's ratio
P-1	24.25±0.81	0.358±0.01	0.385±0.01	7.012±0.08	1.075±0.04
P-2	23.28±0.25	0.528±0.01	0.582±0.02	9.278±0.51	1.102±0.07
P-3	25.98±1.63	0.516±0.02	0.559±0.03	7.692±0.30	1.083±0.03
P-4	24.70±0.58	0.621±0.05	0.659±0.05	5.766±0.31	1.061±0.07
P-5	26.38±1.65	0.543±0.02	0.584±0.04	7.020±0.48	1.075±0.04
P-6	26.55±0.32	0.329±0.01	0.359±0.02	8.356±0.26	1.091±0.05
P-7	25.49±1.27	0.529±0.03	0.567±0.04	6.701±0.14	1.071±0.02
P-8	24.67±0.51	0.781±0.02	0.835±0.07	6.467±0.16	1.069±0.01
P-9	23.51±1.32	0.642±0.05	0.697±0.05	7.890±0.21	1.085±0.02
Values in mean ±SD; n (3)					

Table 9: Post-compression constraints of PZS core tablets.

Formulation	Weight uniformity (mg)	Hardness (kg/cm^2)	Loss on friability (%)	Disintegration time (min)	Drug content (%)
P-1	104.22±2.35	5.32±0.22	0.585±0.02	9.12±0.12	101.55±9.68
P-2	103.24±3.38	6.54±0.62	0.725±0.01	9.28±0.04	101.02±8.58
P-3	105.98±5.69	7.16±0.28	0.599±0.03	6.62±0.05	100.28±6.38
P-4	104.77±6.38	8.21±0.11	0.057±0.01	7.06±0.62	99.26±8.29
P-5	106.84±8.58	9.45±0.32	0.571±0.01	9.00±0.18	98.07±9.68
P-6	104.56±9.65	8.29±0.15	0.399±0.02	8.56±0.13	99.28±8.05
P-7	103.47±8.78	6.52±0.47	0.577±0.01	10.70±0.17	100.23±6.06
P-8	104.85±8.02	8.81±0.65	0.908±0.02	8.46±0.19	101.27±5.08
P-9	104.08±7.18	6.62±0.21	0.597±0.01	12.89±0.08	102.38±8.09
Values in mean ±SD; n (3)					

Table 10: Physicochemical analysis of copious polymer covering films

Formulation	Coat solubility (pH)		Thickness of the film (mm)
	1.2	6.8	
PC-1	Insoluble	Soluble	0.24±0.02
PC-2			0.35±0.02
PC-3			0.29±0.02
PC-4			0.34±0.01
PC-5			0.25±0.02
PC-6			0.38±0.01
PC-7			0.32±0.02
PC-8			0.37±0.01
PC-9			0.22±0.01
Values in mean ±SD; n (3)			

Table 11: ANOVA for the PZS mini-tablets

Source	Sum of Squares	F-value	p-value
Model	0.0266	11.07	0.0377
A-EL100	0.0148	30.81	0.0115
B-CAP	0.0015	3.19	0.1719
AB	0.0009	1.88	0.2643
A^2	0.0049	10.32	0.0489
B^2	0.0092	19.19	0.0220

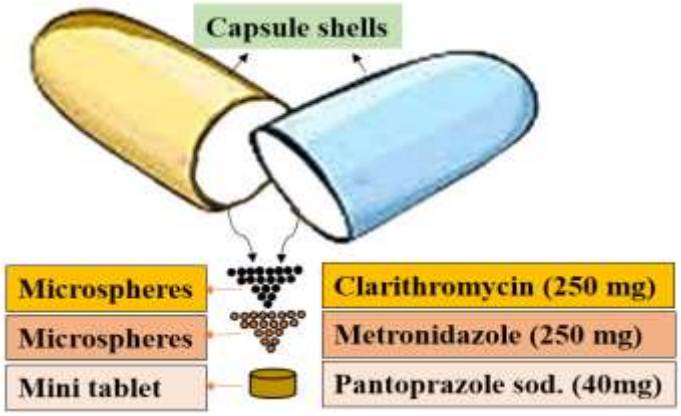

Fig. 1: Hard gelatin capsule filled with CMN and MNZ microspheres and an ECDF of PZS.

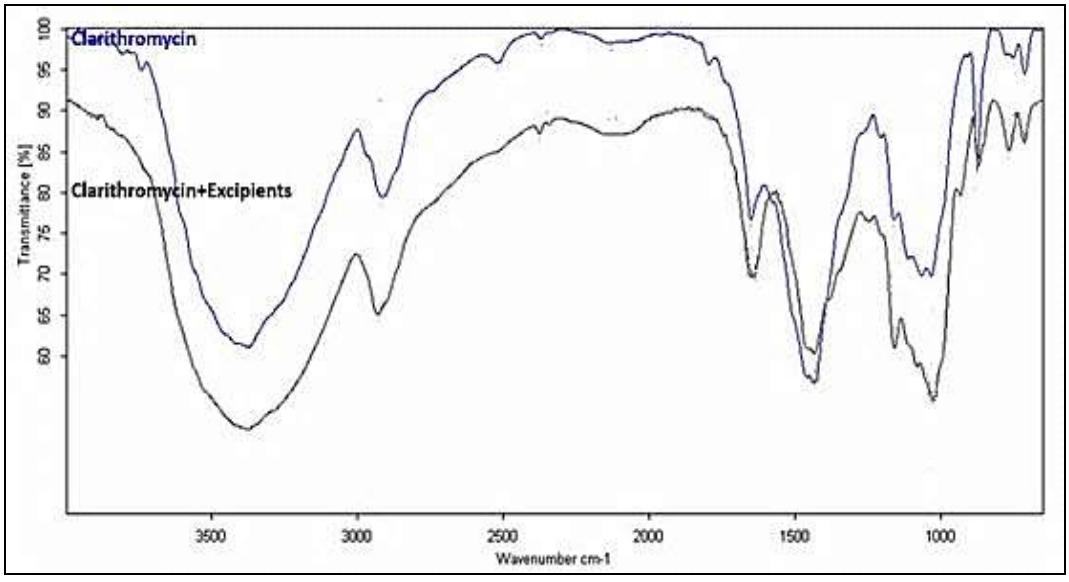

Fig. 2: FTIR spectrum of CMN and CMN+ Excipients.

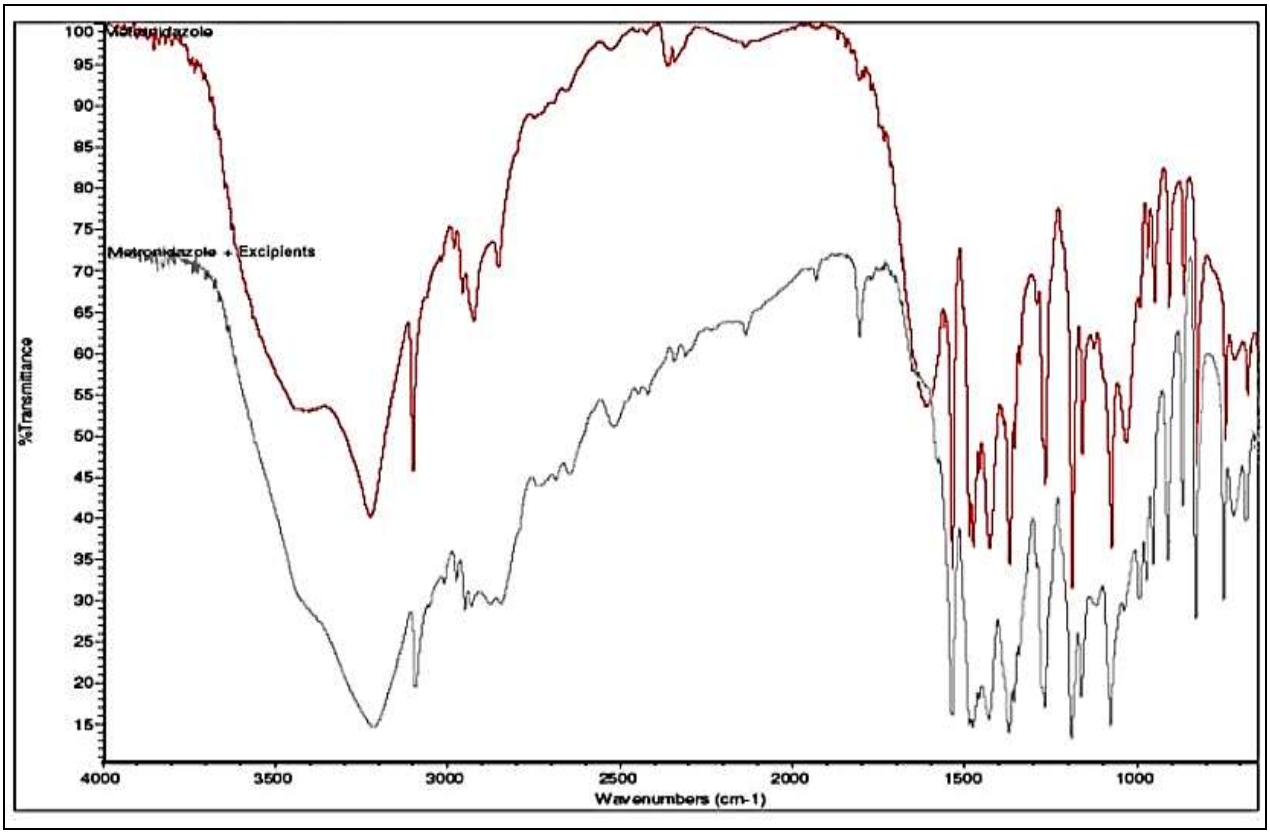

Fig. 3: FTIR spectrum of MNZ and MNZ + excipients

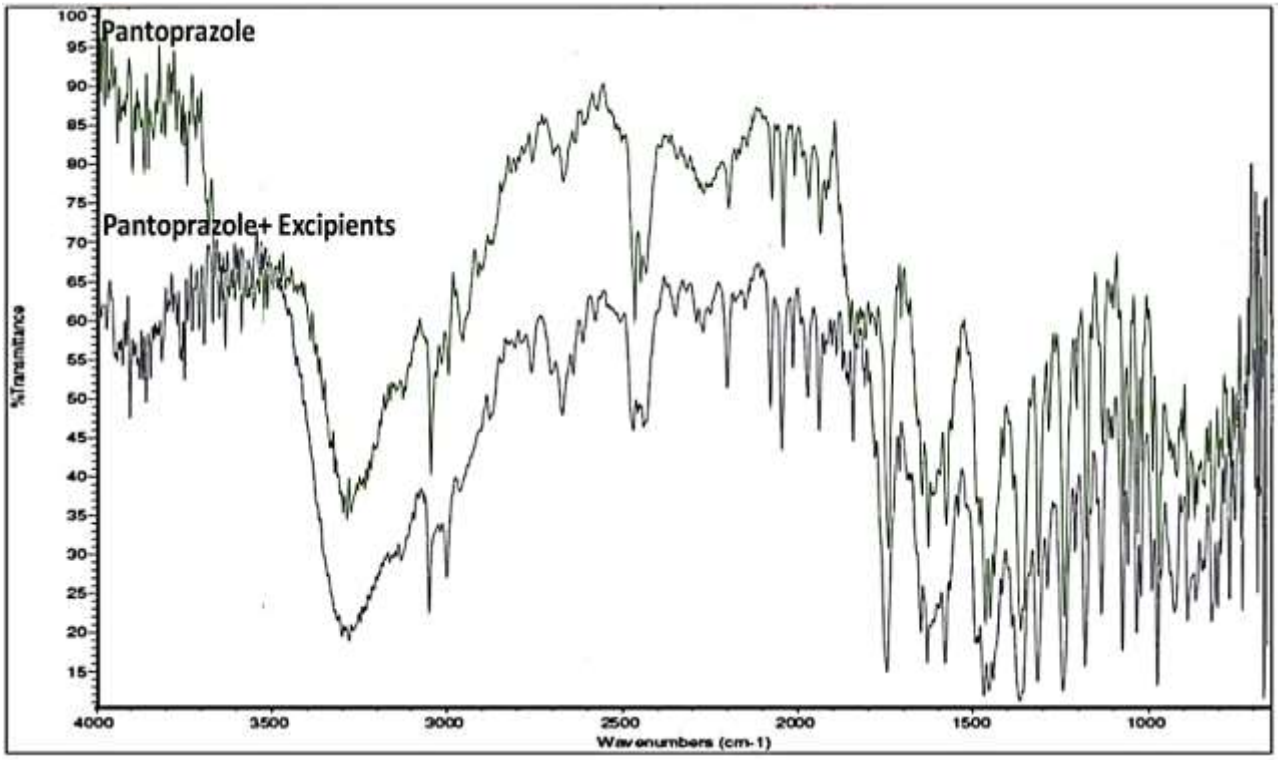

Fig. 4: FTIR spectrum of PZS and PZS+ excipients

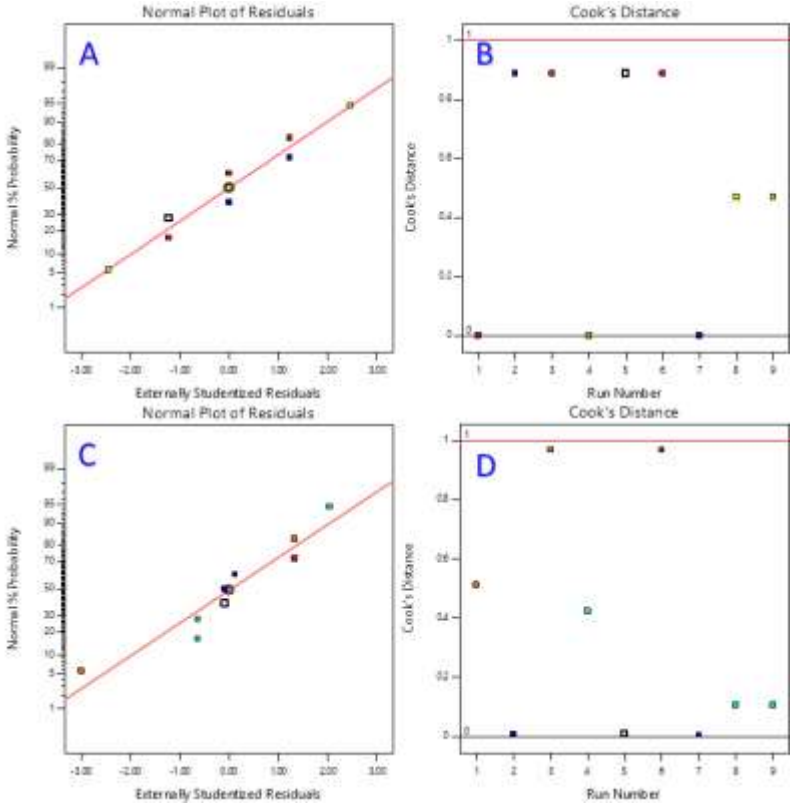

Fig. 5: A-D: Plots of interrelate impact of POSM on the DEE (A&B) and the FT (C&D) for MPFM

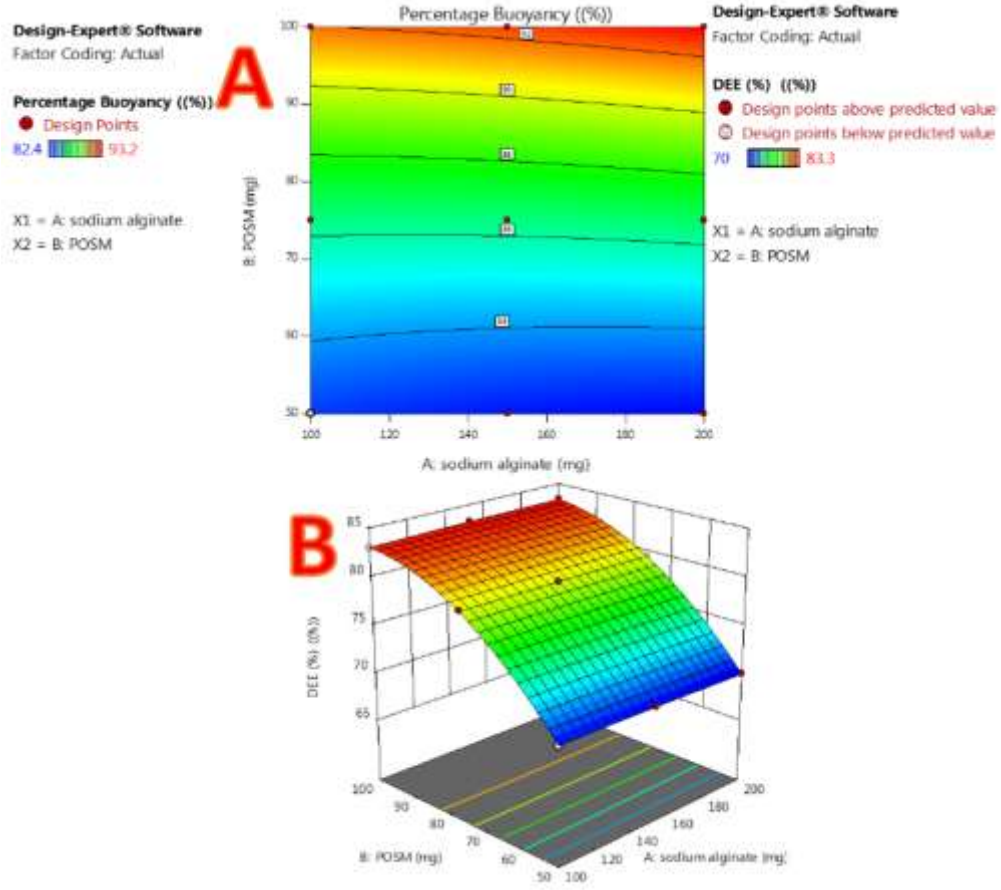

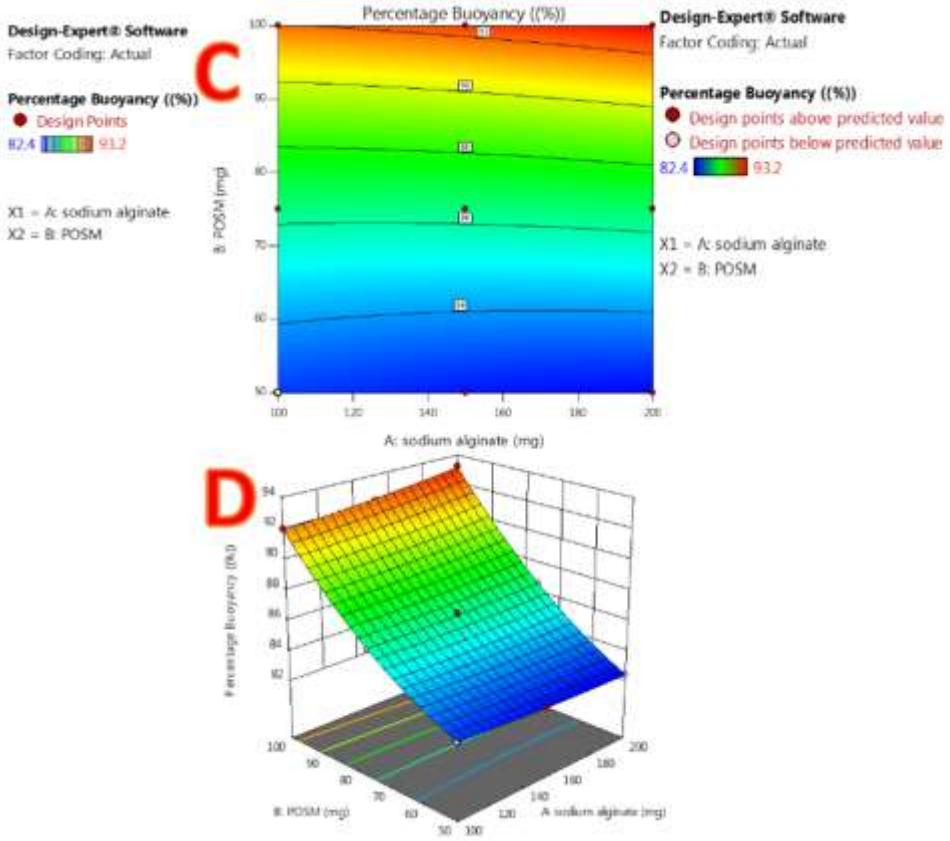

Fig. 6: Contour plot and 3D plot for DEE (A&B) and FT (C&D) for MPFM

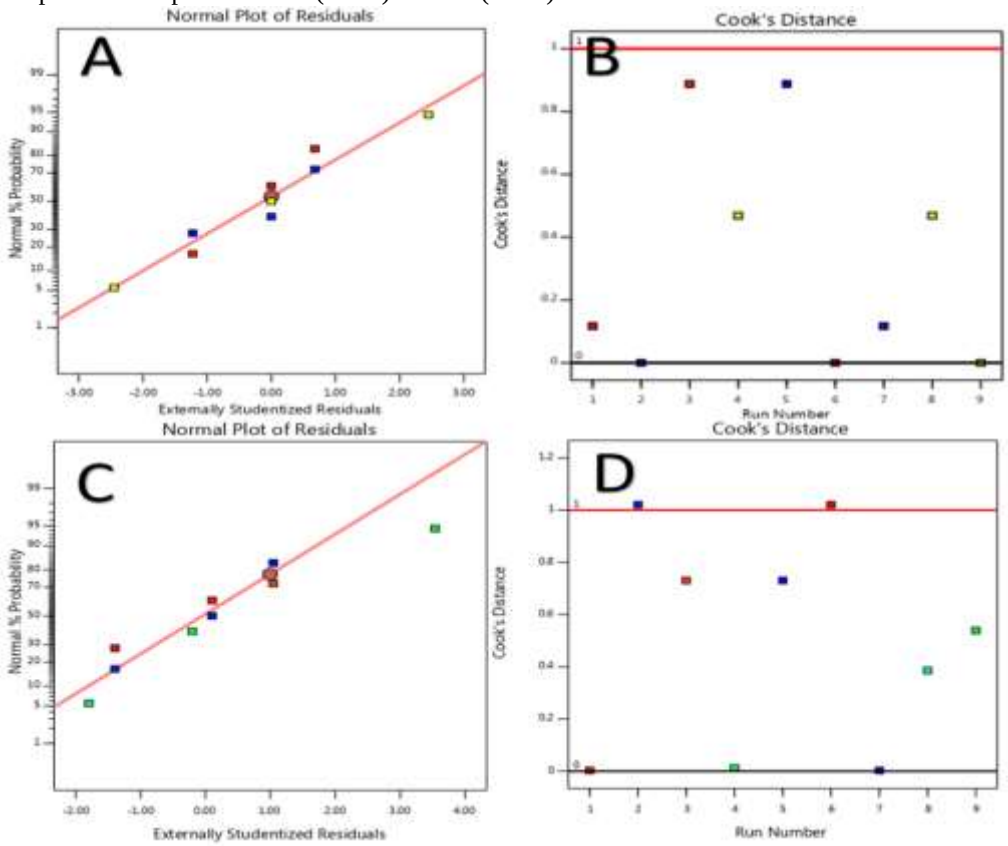

Fig. 7: Plots of the interaction of AEFM on the DEE (A & B,) and the FT (C &D) for CAFM

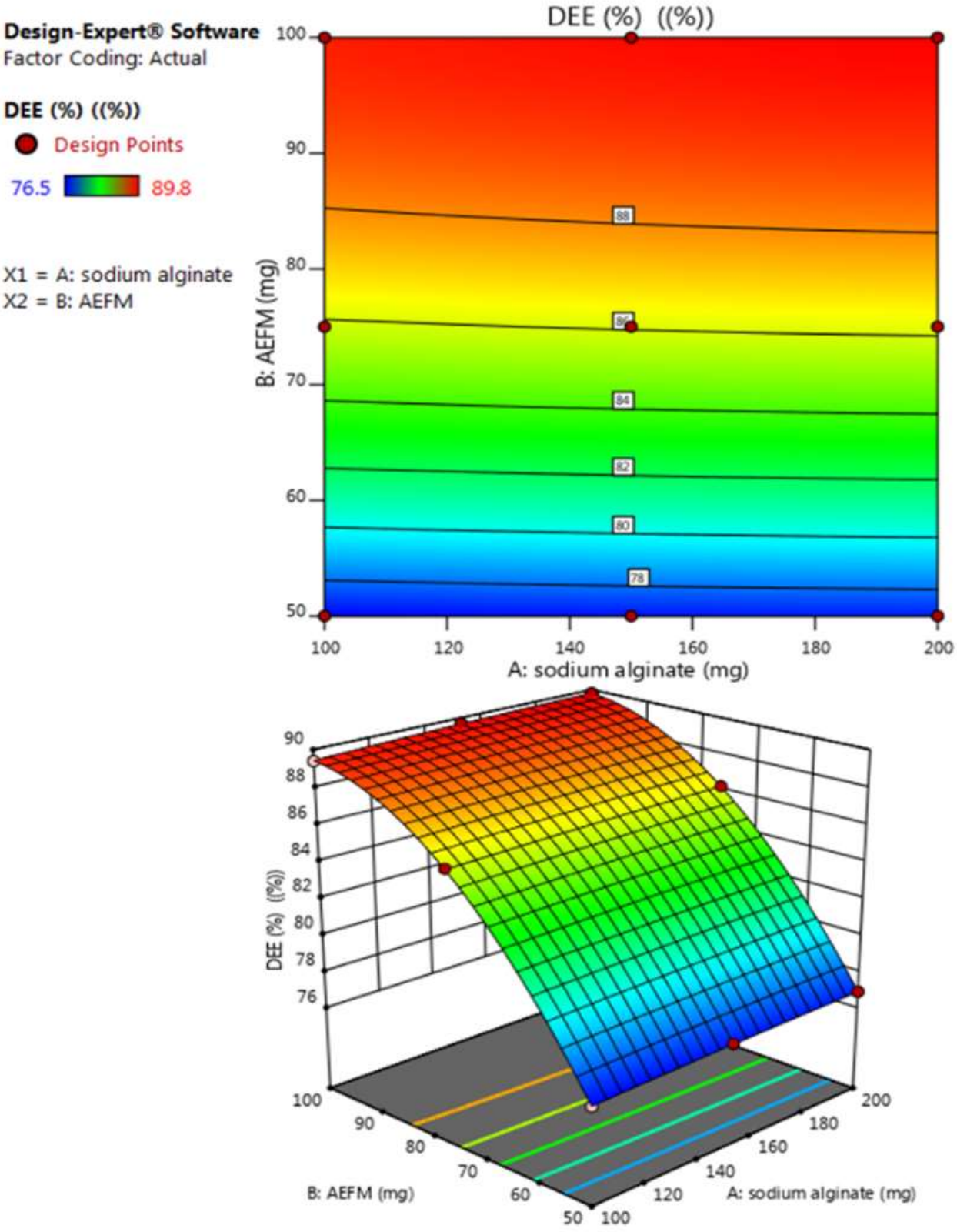
Design-Expert® Software
Factor Coding: Actual
DEE (%) ((%))
Design Points
76.5
89.8
X1 = A: sodium alginate
X2 = B: AEFM
DEE (%) ((%))
B: AEFM (mg)
A: sodium alginate (mg)
DEE (%) ((%))
B: AEFM (mg)
A: sodium alginate (mg)

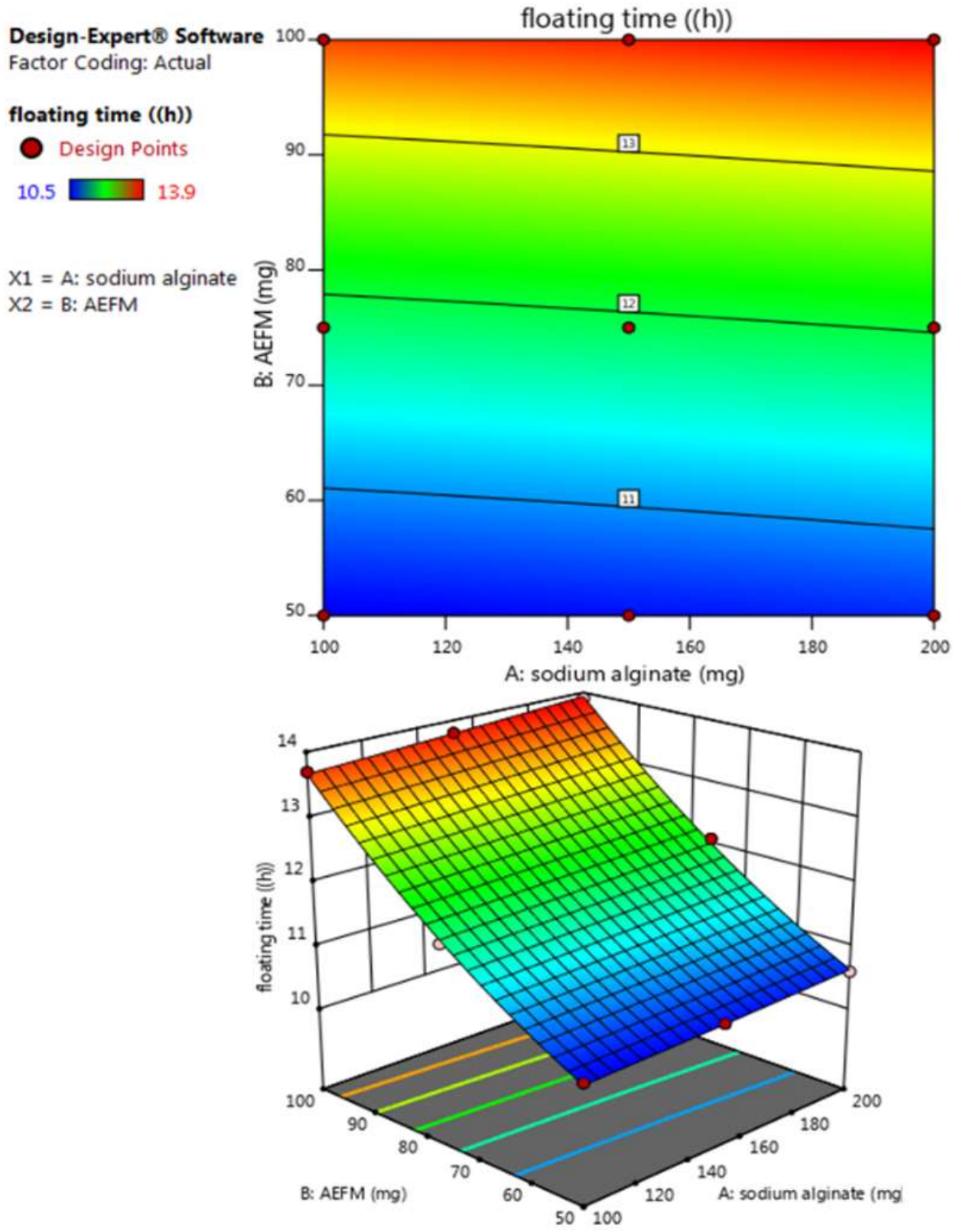

Fig. 8: Contour and 3D plots for DEE (top) and FT (bottom) for CAFM

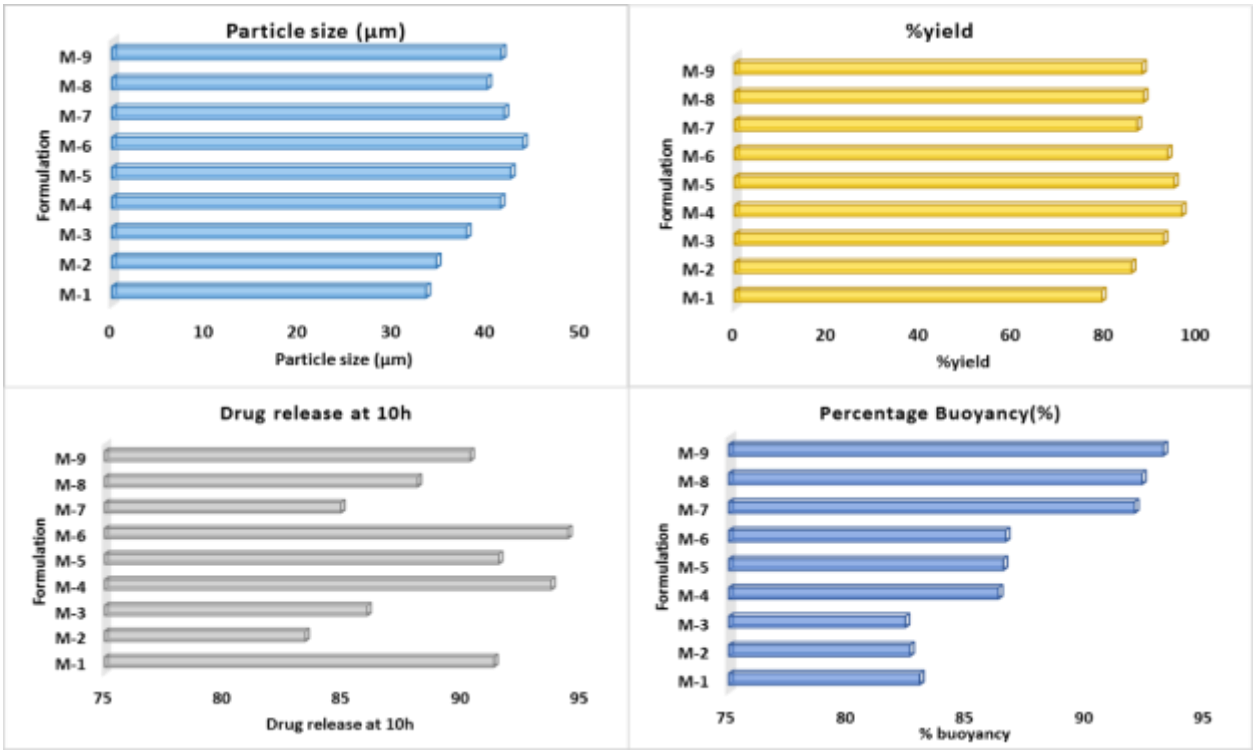

Fig. 9: PS, % yield, MNZ discharge at 10h and % buoyancy of MPFM

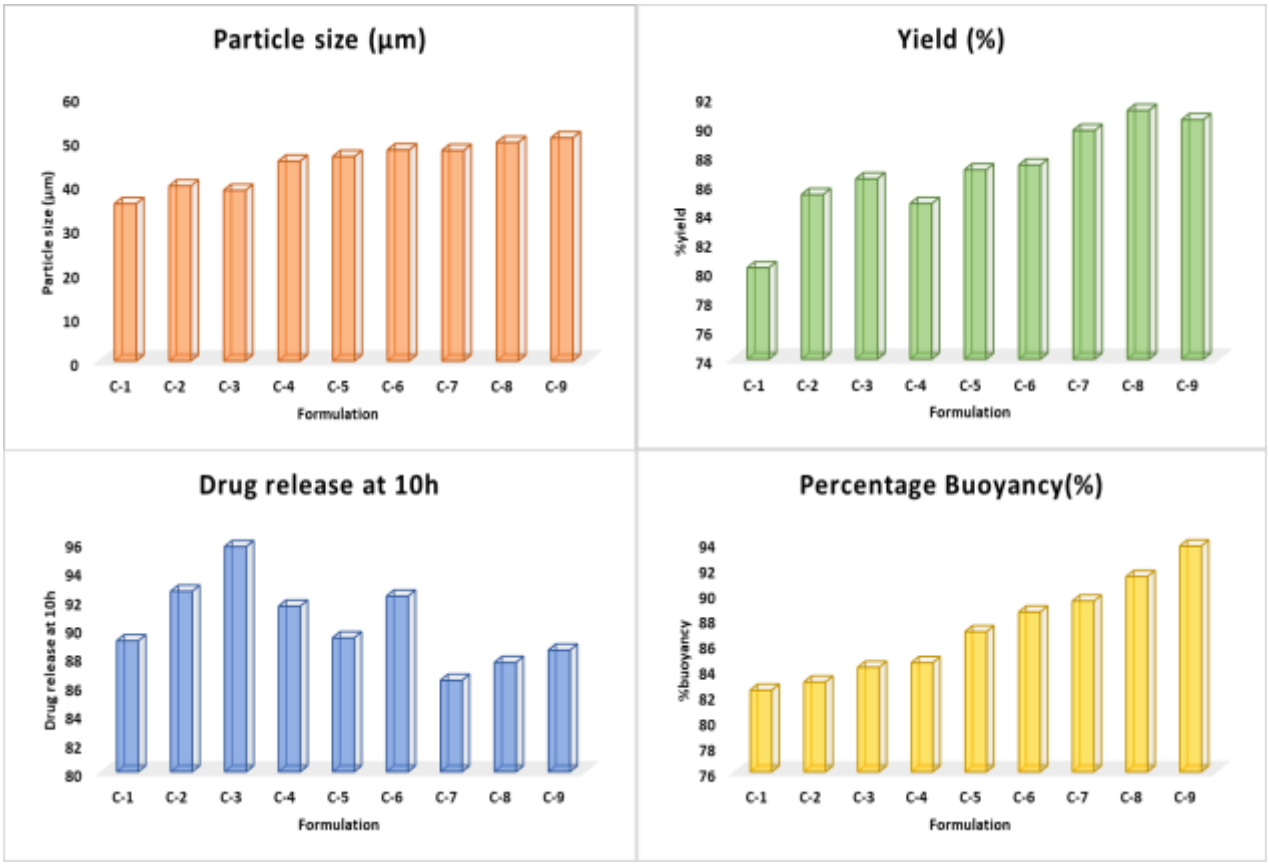

Fig. 10: PS, % yield, CMN discharge at 10h and % buoyancy of CAFM

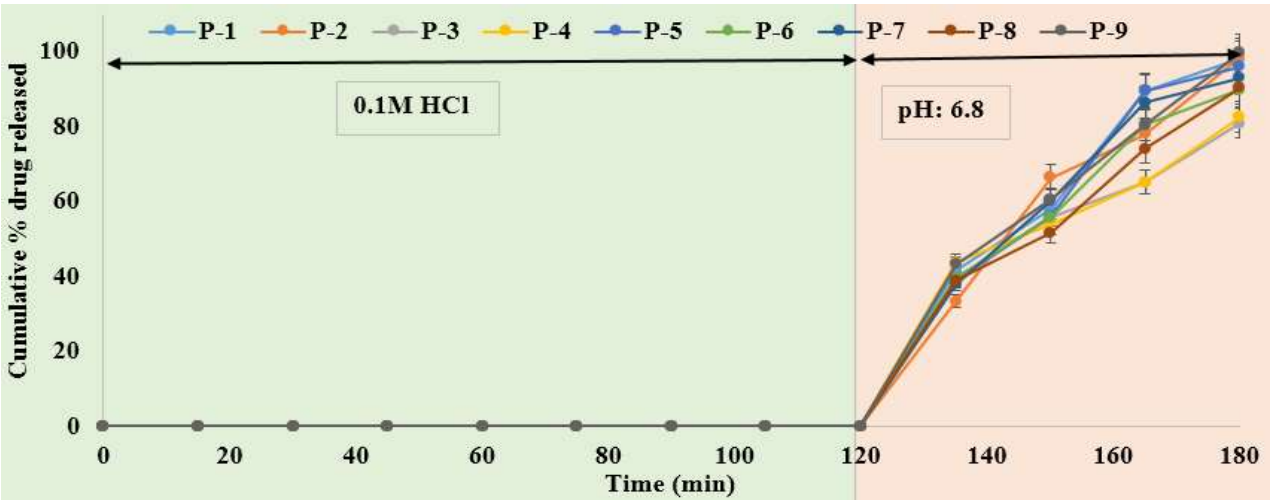

Fig. 11: *In vitro* drug discharge of PZS from the ECDF

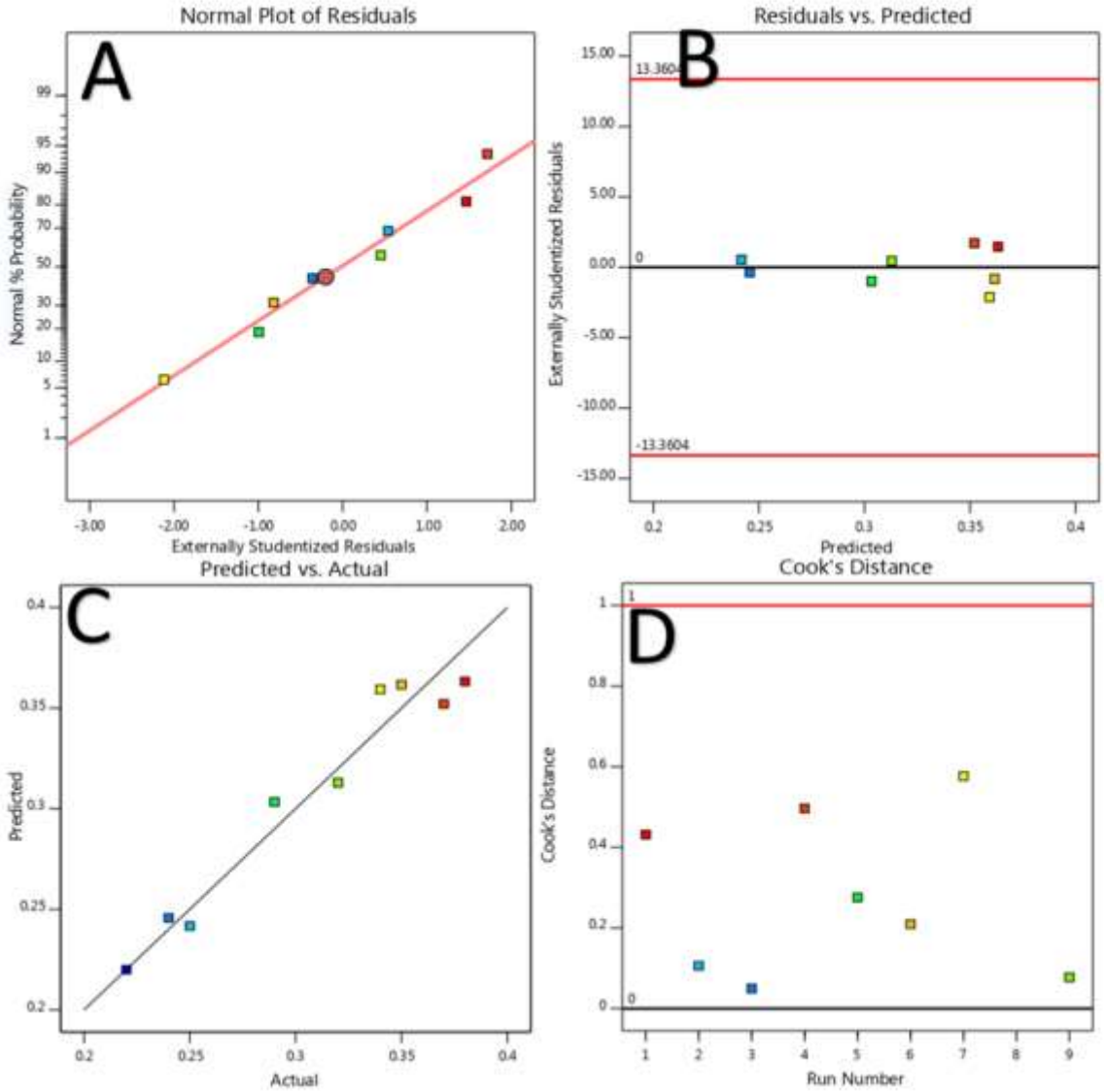

Fig. 12: Plots of the interaction of polymers on the coating thickness for PZS mini-tablets

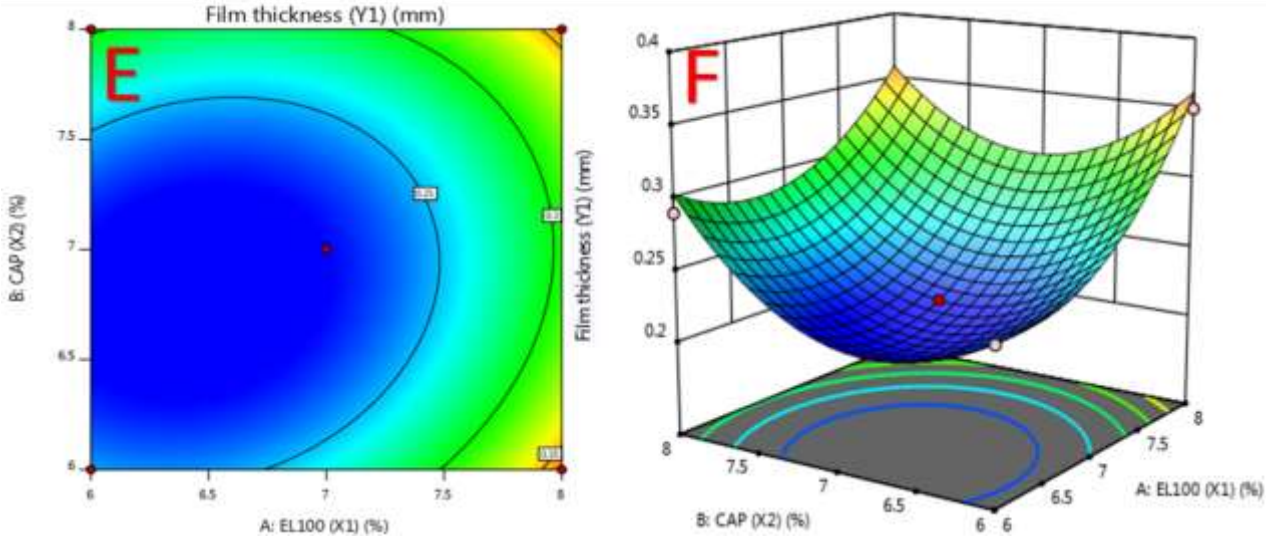

Fig. 13: Contour and 3D plots of coat thickness for PZS mini-tablets

CONCLUSION

The discharge of metronidazole (MNZ) was controlled by a floating polymer in the micro spheres. The formulations float better and discharge MNZ when sodium alginate and *Plantago ovata* seed mucilage (POSM) were combined. F-9 was perceived to be more successful at retaining MNZ than other formulations. Because the POSM amounts in Formulas M-1 to M-3 are less, they have more drug traps. According to the findings, when the amount of POSM in the micro spheres grew, the MNZ trap was revamped and the floating time (FT) was amplified in micro spheres with additional POSM. In micro spheres with higher levels of POSM, MNZ discharge was marginally reduced. According to the exploration, MNZ may be kept in the stomach for a long spell to destroy *H. pylori* and POSM boosted the drifting abilities.

The pace and quantity of Clarithromycin (CMN) discharge are controlled by drifting polymers in the floating drug delivery system. The addition of sodium alginate and *Abelmoschus esculentus* fruit mucilage (AEFM) to the formulations revamped drifting and CMN discharge. C-9 produced better results when compared to other formulas. Drug trapping was better in formulas C-1 to C-3 since the AEFM quantity is less. In all batches, there was a negative connection between revamped floating time and higher AEFM content. Floating microspheres holding AEFM and sodium alginate, according to the study, may revamp CMN retention in the stomach.

From the consistent findings obtained from the research, PZS can be delivered as an ECDF utilizing eudragit L 100 and CAP. Both the polymer and the PZS can protect the PZS from the acidic gastric pH region and discharge it once the intestinal pH is reached. In this exploration, both polymers were used as EC polymers and the best formulation was used. CAP and EudragitL100 were used at 6 % and 6 %, respectively. According to the dissolution, the enteric coat remained stable for 2 h in a pH 1.2 buffer. The optimal formulation is P-1, which is coated with 96.6 % CAP and eudragit L, respectively.

As an import of the research, it was discovered that MNZ microspheres (anti-protozoal), CMN microspheres (anti-bacterial) and PZS enteric-coated pills (proton pump inhibitor) can all be used effectively to eradicate *H. pylori*. POSM and AEFM aided the hovering efficacy and ulcer-curing capability of the formulations.

ACKNOWLEDGMENT

The authors feel privileged to thank the Sri Ramachandra Institute of Higher Education and Research (Deemed University), Porur, Chennai, Tamil Nadu, India their support and encouragement.

REFERENCES

Aby ES, Rodin H and Debes JD (2020). Proton pump inhibitors and mortality in individuals with COVID-19. *Am. J. Gastroenterol.*, **115**(11): 1918-1918.

Ahad HA, Chinthaginjala H, Bhupalam P, Dasari RR, Rao BS and Tarun K (2021). Designing of dexamethasone sodium phosphate ocular films for madras eye: *In vitro* and *in vivo* evaluation. *Pak. Jour. Pharma. Sci.*, **34**(2): 607-613.

Ahad HA, Haranath C, Rahul Raghav D, Gowthami M, Naga Jyothi V and Sravanthi P (2019). Overview on recent optimization techniques in gastro retentive

microcapsules by factorial design. *Int. J. Pharm. Sci Res.*, **10**(9): 247-254.

Ahad HA, Haranath C, Varam NJ, Ksheerasagare T, Krishna JV and Teja ST (2021). Liver shielding activity of *Ficus benghalensis* fruit extracts contrary to perchloromethane prompted toxic hepatitis in New Zealand albino rats. *Res. J. Pharm. Technol.,* **14**(7): 3739-3743.

Ahmad R, Hailat M, Zakaraya Z, Al Meanazel O and Abu Dayyih WJA (2022). Development and validation of an HPLC method for the determination of meloxicam and pantoprazole in a combined formulation. *Analytica*, **3**(2): 161-177.

Ahmed MM (2019). Effect of different formulation variables on release characteristics of gastro-floating microspheres of ethyl cellulose/carbopol 934P encapsulating sorafenib. *Int. J. Pharm. Pharm. Sci.*, **11**(10): 64-70.

Annepogu H, Ahad HA and Nayakanti D (2020). Determining the best poloxamer carrier for thiocolchicoside solid dispersions. *Turk. J. Pharm. Sci.*, **17**(4): 372-380.

Arrua EC, Sanchez SV, Trincado V, Hidalgo A, Quest AF, Morales JOJC and Biointerfaces SB (2022). Experimental design and optimization of a novel dual-release drug delivery system with therapeutic potential against infection with *Helicobacter pylori*. *Colloids Surf. B Biointerfaces,* **213**(5): 112403.

Babu GN, Menaka M and Ahad HA (2022). Neem fruit mucilage-aided mucoadhesive microspheres of acyclovir using 3^2 factorial design with design-expert software. *Appl. Biol. Res.*, **24**(1): 17-27.

Cardos IA, Zaha DC, Sindhu RK and Cavalu S (2021). Revisiting therapeutic strategies for *H. pylori* treatment in the context of antibiotic resistance: focus on alternative and complementary therapies. *Molecules*, **26**(19), 6078-6088.

Charitos IA, D'Agostino D, Topi S and Bottalico L (2021). 40 Years of *Helicobacter pylori*: A revolution in biomedical thought. *Gastroenterol. Insights,* **12**(2): 111-135.

Chen Z, Gan F, Rao X, Huang X and Chen H (2021). Pharmacokinetics, bioequivalence and safety studies of pantoprazole sodium enteric- coated tablets in healthy subjects. *Clin. Pharmacol. Drug Dev*., **10**(5): 502-509.

Chinthaginjala H, Ahad HA, Pradeepkumar B, Gandhi KS, Kalpana K, Pushpalatha G and Sumala K (2021). Formulation and *in vitro* evaluation of gastroretentive ofloxacin floating tablets using natural polymers. *Res. J. Pharm. Technol.*, **14**(2): 851-856.

Das S, Nandi G and Ghosh LK (2019). Okra and its various applications in drug delivery, food technology, health care and pharmacological aspects-a review. *J. Pharm. Sci. Res.*, **11**(6): 2139-2147.

Ejeta F, Gabriel T, Joseph NM and Belete A (2022). Formulation, optimization and *in vitro* evaluation of fast disintegrating tablets of salbutamol sulphate using a combination of superdisintegrant and subliming agent. *Curr. Drug Deliv.*, **19**(1): 129-141.

El Nashar NF, Donia AA, Mady OY and El Maghraby GM (2017). Formulation of clarithromycin floating microspheres for eradication of *Helicobacter pylori. J. Drug Deliv. Sci. Technol.,* **41**(10): 213-221.

Gong L, Yu M, Sun Y, Gao Y, An T, Zou M and Cheng G (2018). Design and optimization of gastric floating sustained-release mini-tablets of alfuzosin hydrochloride based on a factorial design: *In vitro*/*in vivo* evaluation. *Drug Dev. Ind. Pharm.,* **44**(12): 1990-1999.

Gong M, Han Y, Wang X, Tao H, Meng F, Hou B and Wang G (2021). Effect of temperature on metronidazole resistance in *Helicobacter pylori*. *Front. Microbiol.*, **12**(5): 681911.

Hardikar S and Bhosale A (2018). Formulation and evaluation of gastro retentive tablets of clarithromycin prepared by using novel polymer blend. *Bull. Fac. Pharm. Cairo Univ.,* **56**(2): 147-157.

Harsha SS, Ahad HA, Haranath C, Dasari RR, Gowthami M, Varam NJ and Musa G (2020). Exfoliation technique of composing and depictions of clopidogrel bisulphate afloat microspheres. *J. Evol. Med. Dent. Sci.*, **9**(14): 1156-1161.

Hindustan AA, Babu UA, Nagesh K, Kiran DS and Madhavi KB (2012). Fabrication of glimepiride datura stramonium leaves mucilage and poly vinyl pyrrolidone sustained release matrix tablets: *In vitro* evaluation. *KUSET*, **8**(1): 63-72.

Islam MT (2019). Phytochemical information and pharmacological activities of Okra (Abelmoschus esculentus): A literature- based review. *Phytother. Res.*, **33**(1): 72-80.

Ismail A, Raafat E and Sakran W (2022). Statistically-based optimization of verapamil hydrochloride loaded gastroretentive alginate beads. *J. Adv. Pharm. Res.*, **6**(4): 207-222.

Israr M, Pugliese N, Farid A, Ghazanfar S, Di Cerbo A, Muzammal M and Khan KA (2022). Preparation and characterization of controlled-release floating bilayer tablets of esomeprazole and clarithromycin. *Molecules*, **27**(10): 3242.

Kan LD, Chen J, Huang YT, Qiu Y, Yu XL, Fang HM, Li LC (2020). Evaluation of different proton pump inhibitors combined with bismuth quadruple regimens in *Helicobacter pylori* eradication. *Exp. Clin. Med.*, **20**(4): 609-614.

Keshavarzi S, Sepehrimanesh M, Mirzaei B, Koohi-Hosseinabadi O, Sardari Z and Sajjadpur MM (2021). Antimicrobial effects of aqueous and hydro-alcoholic plantago psyllium leaf extracts on the experimental infection of *Helicobacter pylori* in a rat model. *J. Adv. Med. Biomed. Res.*, **29**(137): 317-323.

Khan WA and Alishah SH (2022). *H. pylori* infection in human gastrointestinal cancer diagnosis and treatment

control: A review. *Int. J. Adv. Res. Biol. Sci.*, **9**(7): 108-19.

Krag M, Marker S, Perner A, Wetterslev J, Wise MP, Schefold JC and Borthwick M (2018). Pantoprazole in patients at risk for gastrointestinal bleeding in the ICU. *N. Engl. J. Med.*, **379**(23): 2199-2208.

Le XT, Nguyen HM, Le NQ and Trinh TTL (2021). Formulation of enteric coated microspheres containing pantoprazole. *VJSTE*, **63**(3): 56-62.

Lin YH, Lin JH, Chou SC, Chang SJ, Chung CC, Chen YS and Chang CH (2015). Berberine-loaded targeted nanoparticles as specific *Helicobacter pylori* eradication therapy: *In vitro* and *in vivo* study. *Nanomedicine*, **10**(1), 57-71.

Liu Q, Meng X, Li Y, Zhao CN, Tang GY, Li S and Li HB (2018). Natural products for the prevention and management of *Helicobacter pylori* infection. *Compr. Rev. Food Sci. Food Saf.*, **17**(4): 937-952.

Maderuelo C, Lanao JM and Zarzuelo A (2019). Enteric coating of oral solid dosage forms as a tool to improve drug bioavailability. *Eur. J. Pharm. Sci.*, **138**(10): 105019.

Malladi M and Jukanti R (2016). Formulation development and evaluation of a novel bi-dependent clarithromycin gastroretentive drug delivery system using Box-Behnken design. *J. Drug Deliv. Sci. Technol.*, ***35***(10): 134-145.

Moussa BA, El-Kady EF, Mohamed MF and Youssef NF (2017). Greener thin-layer chromatographic solvents for the determination of pantoprazole sodium sesquihydrate, metronidazole and clarithromycin in pharmaceutical formulations used as triple therapy in Helicobacter infection. *JPC-J Planar. Chromat.*, **30**(6): 481-487.

Oladeji SA, Dadou SM, Zhao M, Li S, Jones DS and Andrews GP (2022). The development and optimisation of gastro-retentive floating tablets using fused deposition modelling 3D printing. *J. Pharm. Pharmacol*., **74**(10): 1450-1466.

Paul B, Adimoolam S and Qureshi MJ (2018). Development and evaluation of metronidazole loaded carbopol 934P mucoadhesive microcapsules for sustained drug release at the gastric mucosa. *J. Appl. Pharm. Sci.*, **8**(12): 020-031.

Rajora A and Nagpal K (2022). A critical review on floating tablets as a tool for achieving better gastric retention. *Crit. Rev. Ther. Drug Carrier Syst.*, **39**(1): 65-103.

Raza A, Shen N, Li J, Chen Y and Wang JY (2019). Formulation of zein based compression coated floating tablets for enhanced gastric retention and tunable drug release. Eur. J. Pharm. Sci., **132**(4): 163-173.

Schubert JP, Warner MS, Rayner CK, Roberts- Thomson IC, Mangoni AA, Costello S and Bryant RV (2022). Increasing *Helicobacter pylori* clarithromycin resistance in Australia over 20 years. *J. Intern. Med.*, **52**(9): 1554-1560.

Shapla UM, Raihan J, Islam A, Alam F, Solayman N, Gan SH and Khalil I (2018). Propolis: The future therapy against *Helicobacter pylori* – mediated gastrointestinal diseases. *J. Appl. Biomed.*, **16**(2): 81-99.

Soisuwan S, Teeranachaideekul V, Wongrakpanich A, Langguth P and Junyaprasert VB (2018). *In vitro* performances and cellular uptake of clarithromycin nanocrystals produced by media milling technique. *Powder Technol.*, **338**(10): 471-480.

Sowjanya HBM and Ahad HA (2022). Mastic gum aided amoxicillin trihydrate gastro retentive mucoadhesive microspheres: *In vivo* evaluation. *Bangladesh J. Sci. Ind. Res.*, **57**(3): 187-194.

Spugnini EP and Fais S (2020). Drug repurposing for anticancer therapies. A lesson from proton pump inhibitors. *Expert Opin. Ther. Pat.*, **30**(1): 15-25.

Stephin J and Marina K (2020). Preparation and investigation of gastro-retentive mucoadhesive microspheres of clarithromycin-resin complex. *Int. J. Pharm. Investig*., **10**(4): 445-451.

Thombre NA and Gide PS (2016). Floating-bioadhesive gastroretentive Caesalpinia pulcherrima-based beads of amoxicillin trihydrate for *Helicobacter pylori* eradication. *Drug Deliv.*, **23**(2): 405-419.

Zhang S, Fang M, Zhang Q, Li X, Zhang TJDD and Pharmacy I (2019). Evaluating the bioequivalence of metronidazole tablets and analyzing the effect of *in vitro* dissolution on *in vivo* absorption based on PBPK modeling. *Drug Dev. Ind. Pharm.*, **45**(10): 1646-1653.